

<https://doi.org/10.1038/s41698-025-00912-x>

# Enhanced efficacy of ipilimumab plus nivolumab in angiogenic subtypes of metastatic clear-cell renal cell carcinoma

Check for updates

Xiaofan Lu<sup>1,8</sup>, Yann-Alexandre Vano<sup>2,3,8</sup>, Xiaoping Su<sup>4,8</sup>, Virginie Verkarre<sup>5</sup>, Cheng-Ming Sun<sup>3</sup>, Wenxuan Cheng<sup>1</sup>, Li Xu<sup>1</sup>, Fangrong Yan<sup>6</sup>, Salma Kotti<sup>2</sup>, Wolf Herman Fridman<sup>3</sup>, Catherine Sautes-Fridman<sup>3</sup>, Stéphane Oudard<sup>2,9</sup>✉ & Gabriel G. Malouf<sup>1,7,9</sup>✉

In metastatic clear-cell renal cell carcinoma (mccRCC), choosing between immuno-oncology (IO) combinations and IO plus anti-VEGF therapies is uncertain. The BIONIKK trial revealed that ipilimumab plus nivolumab (Ipi/Nivo) achieved a 70% objective response rate in angiogenic cluster1/2 versus 41% in cluster4/5, which featured T-effector/cell-cycle signatures ( $p = 0.048$ ). Complete responses were exclusively observed in cluster1/2 ( $p = 0.012$ ), with longer progression-free survival ( $p = 0.014$ ). Ipi/Nivo may particularly benefit angiogenic mccRCC, supporting molecular subtype-based treatment strategies.

The first-line treatment for metastatic clear cell renal cell carcinoma (mccRCC) includes immuno-oncology (IO) based combination therapies. As per the NCCN guidelines (v1.2025), the standard treatment involves a PD-1 inhibitor combined with either an anti-CTLA-4 inhibitor (e.g., ipilimumab + nivolumab [Ipi/Nivo]) or an anti-vascular endothelial growth factor receptor tyrosine kinase inhibitor (TKI) (e.g., axitinib + pembrolizumab [Axi/Pembro], cabozantinib + nivolumab [Cabo/Nivo], lenvatinib + pembrolizumab)<sup>1</sup>. These combinations are preferred for all patient populations irrespective of International Metastatic RCC Database Consortium (IMDC) risk categories. Notably, Ipi/Nivo is now preferred across all categories, bolstered by the compelling outcomes from the CheckMate-214 trial (CM214). Despite advancements, clear guidelines to inform the choice between IO/IO and IO/TKI combinations are lacking.

Molecular profiling of 823 ccRCC tumors in the phase III IMmotion 151 (IM151) trial identified seven biologically distinct gene expression clusters. The analysis indicated that atezolizumab combined with bevacizumab (IO/TKI, not yet FDA approved) was particularly effective in subsets characterized by high angiogenesis (cluster1/2) and in those with elevated T-effector and/or cell-cycle transcription signatures (cluster4/5)<sup>2</sup>. These insights have motivated the design of clinical trials like the phase II OPTIC RCC trial, a pioneering biomarker-driven study that assigns patients to IO/TKI (Cabo/Nivo) for cluster1/2 or IO/IO (Ipi/Nivo) for cluster4/5<sup>3</sup>.

However, unexpected findings emerged from the BIONIKK trial—a phase II biomarker-driven study in mccRCC guided by the Descartes classifications (ccrcc1 to ccrcc4). This trial demonstrated a notably higher overall response rate (ORR) of 51% in the pro-angiogenic ccrcc2 subgroup when treated with Ipi/Nivo. The complete response rate was over five times greater in this subgroup compared to those treated with sunitinib (16% vs. 3%), highlighting a significant deviation from the expected efficacy of VEGF-targeting strategies in angiogenesis-dominant tumors<sup>4</sup>. Within this subgroup, patients exhibiting higher expression of immune genes demonstrated enhanced responsiveness<sup>4</sup>. Furthermore, the application of the IM150 angiogenesis signature ('Angio') effectively predicted the clinical benefit in mccRCC patients receiving the Ipi/Nivo combination<sup>5</sup>, challenging the prevailing notion that high levels of VEGF expression predominantly benefit from TKI-inclusive therapies.

To further explore the efficacy of IO/IO therapy in treating patients with diverse molecular characteristics, particularly those with prominent angiogenic and T-effector/cell-cycle profiles, we analyzed the transcriptomic and clinical landscapes of all 49 patients treated with Ipi/Nivo in the BIONIKK trial who had adequate tumor tissue available for RNA sequencing. Of note, sarcomatoid features were specifically included in the analysis to evaluate their impact on the efficacy of IO/IO therapy, given their association with aggressive disease behavior and potentially differential

<sup>1</sup>Department of Cancer and Functional Genomics, Institute of Genetics and Molecular and Cellular Biology, CNRS/INSERM/UNISTRA, 67400 Illkirch, France.

<sup>2</sup>Department of Medical Oncology, Hôpital Européen Georges Pompidou, Institut du Cancer Paris CARPEM, APHP, Université Paris Cité, Paris, France. <sup>3</sup>Centre de Recherche Cordeliers, INSERM 1138, Université de Paris Cité, Sorbonne Université, Equipe labellisée Ligue contre le Cancer, F-75006 Paris, France. <sup>4</sup>Department of Bioinformatics and Computational Biology, The University of Texas MD Anderson Cancer Center, Houston, TX, USA. <sup>5</sup>Department of Pathology, Hôpital Européen Georges Pompidou, Institut du Cancer Paris CARPEM, APHP, Université Paris Cité, Paris, France. <sup>6</sup>Research Center of Biostatistics and Computational Pharmacy, China Pharmaceutical University, Nanjing, China. <sup>7</sup>Department of Medical Oncology, Strasbourg University, Institut de Cancérologie de Strasbourg, Strasbourg, France. <sup>8</sup>These authors contributed equally: Xiaofan Lu, Yann-Alexandre Vano, Xiaoping Su. <sup>9</sup>These authors jointly supervised this work: Stéphane Oudard and Gabriel G. Malouf. ✉e-mail: [stephane.oudard@aphp.fr](mailto:stephane.oudard@aphp.fr); [maloufg@igbmc.fr](mailto:maloufg@igbmc.fr)

responses to immune checkpoint inhibitors (ICIs)<sup>6</sup>. We established a model-free predictive framework using nearest template prediction based on uniquely upregulated genes previously described for each cluster (Fig. S1, Table S1)<sup>2,7</sup>. This analysis classified the 49 tumors into four clusters, the prediction accuracy of which was supported by both gene-level expression and pathway enrichment analyses (Fig. 1A, Fig. S2)<sup>2,8</sup>. Tumors in clusters 1 (angiogenic/stromal) and 2 (angiogenic) exhibited high levels of vascular pathway genes (*VEGFA*, *CD34*) and showed significant activation of angiogenic and hypoxia-related pathways. Uniquely, cluster 1 featured high degree of fibroblast-derived gene expression, increased expression of collagens and activated stroma-associated genes (*FAP*, *FNI*, *POSTN*, *COL1A1*, *MMP2*), and demonstrated enrichment of epithelial mesenchymal transition pathways, while cluster 2 also showed moderate T-effector gene signature expression, low cell-cycle-associated genes, and higher expression of genes associated with catabolic metabolism, including those in Fatty Acid Oxidation (FAO; *CPT2*, *PPARA*, *CPT1A*) and AMP-activated protein kinase (AMPK; *PRKAA2*, *PDK2*, *PRKAB1*). In contrast, clusters 4 (T-effector/proliferative) and 5 (proliferative) displayed elevated levels of cell cycle genes (*CDK2*, *CCNE1*) with enrichment of proliferation-associated pathways including E2F targets, G2/M checkpoint, and Myc target.

Clusters 4 and 5 also exhibited an anabolic metabolism transcriptomic profile, with higher expression of genes associated with Fatty Acid Synthesis (FAS; *FASN*, *PARP1*) and the pentose phosphate pathway (*TKT*, *TALDO1*, *PGD*), which may be related to the proliferative nature of these tumors. Cluster 4 additionally showed T-cell activation genes (*CD8A*, *IFNG*) and activation of immune-related pathways, particularly inflammatory response and interferon gamma response.

Compared to the Descartes classification upon which the BIONIKK trial was based, cluster 1 was predominantly enriched in Descartes ccrcc1 (83% vs. 27%,  $p = 0.001$ ), characterized by lower immune infiltration. Cluster 2 was enriched in pro-angiogenic ccrcc2 (80% vs. 21%,  $p = 0.0002$ ), and cluster 4 showed a high prevalence of ccrcc4, known for its significant immune and inflammatory activity (50% vs. 3%,  $p = 0.0002$ ). Conversely, cluster 5 exhibited a mixed Descartes classification. Confirming the IM151 findings<sup>2</sup>, the cluster1/2 significantly enriched in IMDC favorable risk group compared to cluster4/5 (15 [56%] vs. 5 [23%],  $p = 0.040$ ), and had lower rate of sarcomatoid component (2 [7%] vs. 6 [27%],  $p = 0.117$ ) (Table 1).

Cluster1/2 exhibited significantly longer progression-free survival time (median survival: 23.2 vs. 10.2 months,  $p = 0.014$ ; Fig. 1B), and a reduced risk of progression compared to cluster4/5 when adjusting for IMDC and

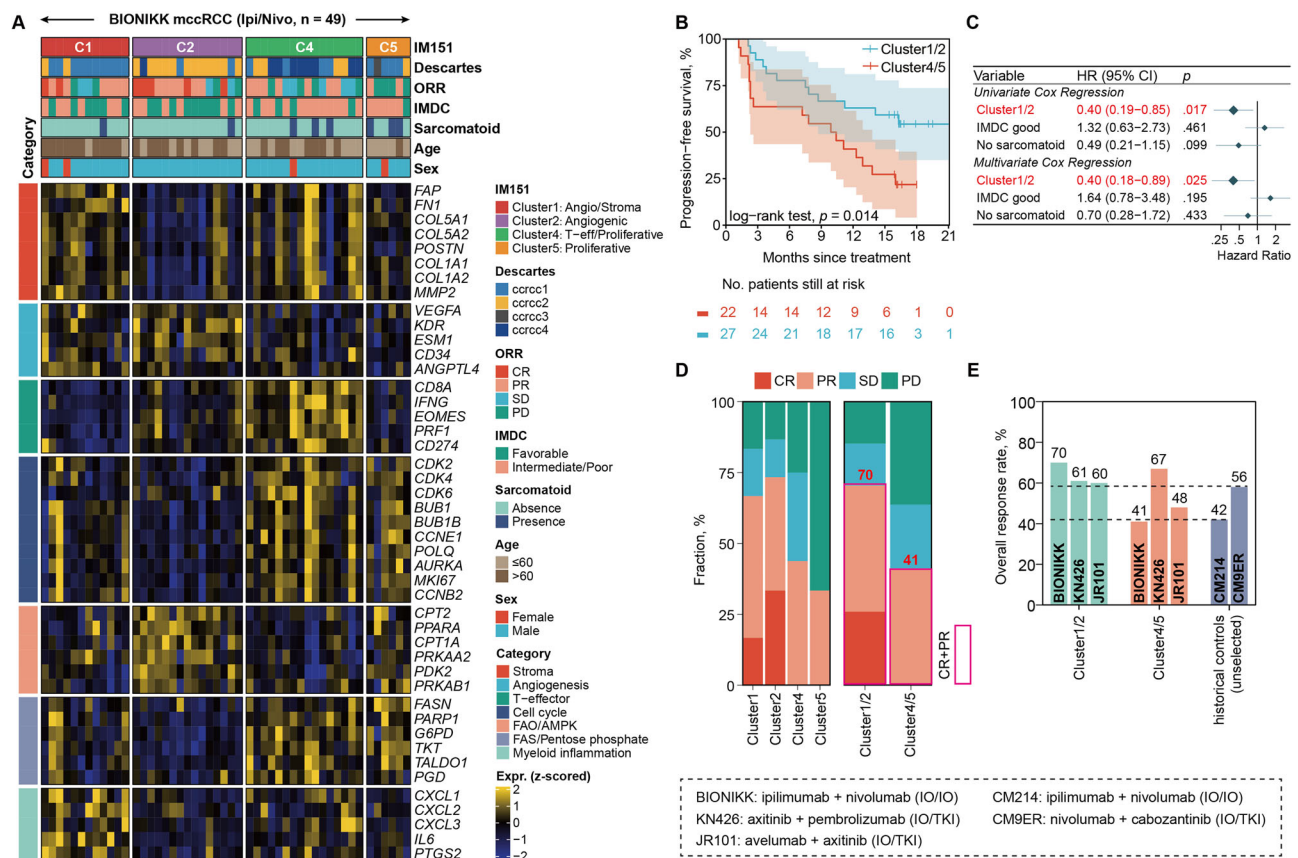


**Fig. 1 | Enhanced efficacy of IO/IO combinations in angiogenic subtypes in the BIONIKK trial.** **A** Heatmap showing gene expression profiles (log2 transformed TPM values, z-scored, truncated to range [-2,2]) of BIONIKK trial tumor samples grouped by NTP-predicted molecular subtypes. Each cluster shows unique features: Cluster 1 exhibits high expression of stromal and angiogenesis-related genes; cluster 2 shows elevated expression of angiogenesis and fatty acid oxidation genes; cluster 4 displays increased expression of T-effector cell and cell cycle/proliferation genes; cluster 5 is marked by upregulation of proliferation-related genes. Patient demographics, International Metastatic Renal Cell Carcinoma Database Consortium (IMDC) risk group, and objective response are annotated at the top of the heatmap. FAO, fatty acid oxidation; FAS, fatty acid synthesis; AMPK, AMP-activated protein kinase. **B** Progression-free survival (PFS) rates stratified by cluster1/2 and cluster4/5. **C** Forest plot displaying hazard ratios (HRs) for PFS by

molecular clusters, IMDC risk, and sarcomatoid status, using univariate and multivariate Cox regression. Reference groups are cluster4/5 for molecular clusters, intermediate/poor risk for IMDC, and sarcomatoid presence. Multivariate analysis confirms the independence of cluster1/2 as a prognostic factor. **D** Distribution of objective responses across molecular subtypes. The upper panel shows distribution in four subgroups, and the bottom panel shows distribution in cluster1/2 versus cluster4/5. Overall responses (complete response + partial response) are framed in plum red. **E** Comparison of overall response rates (ORR) across different treatment arms in renal cell carcinoma trials. This includes the IO/IO arm of the BIONIKK trial, the IO/TKI arms of KEYNOTE-426 (KN426) and JAVELIN Renal 101 (JR101), and unselected historical controls from the CheckMate-214 (CM214) and CheckMate-9ER (CM9ER) trials. CR complete response, PR partial response, SD stable disease, PD progressive disease.

**Table 1 | Patient demographics and clinical characteristics across four molecular clusters of Ipi/Nivo arm of BIONIKK trial**

	Cluster1	Cluster2	Cluster4	Cluster5	<i>P</i> <sub>cluster1/2 vs. 4/5</sub>
No. of sample	12 (24%)	15 (31%)	16 (33%)	6 (12%)	
Age					0.047
≤60	2 (17%)	7 (47%)	9 (56%)	5 (83%)	
>60	10 (83%)	8 (53%)	7 (44%)	1 (17%)	
Sex					1
Female	2 (17%)	0	1 (6%)	1 (17%)	
Male	10 (83%)	15 (100%)	15 (94%)	5 (83%)	
Sarcomatoid					0.117
Absence	11 (92%)	14 (93%)	13 (81%)	3 (50%)	
Presence	1 (8%)	1 (7%)	3 (19%)	3 (50%)	
IMDC					0.040
Favorable	6 (50%)	9 (60%)	4 (25%)	1 (17%)	
Intermediate/Poor	6 (50%)	6 (40%)	12 (75%)	5 (83%)	
ORR					0.029
CR	2 (17%)	5 (34%)	0	0	
PR	6 (50%)	6 (40%)	7 (44%)	2 (33%)	
SD	2 (17%)	2 (13%)	5 (31%)	0	
PD	2 (17%)	2 (13%)	4 (25%)	4 (66%)	
Descartes					0.007
crrcc1	10 (83%)	2 (13%)	4 (25%)	4 (66%)	
crrcc2	2 (17%)	12 (80%)	4 (25%)	1 (17%)	
crrcc3	0	0	0	1 (17%)	
crrcc4	0	1 (7%)	8 (50%)	0	

IMDC International Metastatic Renal Cell Carcinoma Database Consortium, ORR overall response rate, CR complete response, PR partial response, SD stable disease, PD progressive disease.

sarcomatoid status, with an adjusted hazard ratio of 0.40 (95% confidence interval: 0.18–0.89,  $p = 0.025$ ; Fig. 1C). Furthermore, cluster1/2 demonstrated a 70% ORR, substantially higher than the 41% observed in cluster4/5 ( $p = 0.048$ , Fig. 1D). More importantly, all complete responses were exclusively observed in cluster1/2 ( $p = 0.012$ ), highlighting the complex role of angiogenesis in supporting immune responses. The intriguing associations found in CM214 trial suggest complex relationships between angiogenesis and immunotherapy efficacy—while gene sets linked to hypoxia and reactive oxygen species correlated positively with patient outcomes under the Ipi/Nivo regimen, the angiogenesis signature (Angio) was not associated with Ipi/Nivo outcomes<sup>9</sup>. These findings highlight the need to better understand the biological basis for enhanced IO/IO efficacy in angiogenic subtypes.

We further performed a cross-trial analysis comparing IO-based treatment outcomes across molecular subtypes. For trials with available molecular data, we analyzed BIONIKK (Ipi/Nivo), KEYNOTE-426 (Axi/Pembro)<sup>10,11</sup>, and JAVELIN Renal 101 (JR101) (avelumab + axitinib [Ave/Axi])<sup>8,12</sup>. These were compared with unselected population data from CM9ER (Cabo/Nivo)<sup>13</sup> and CM214 (Ipi/Nivo)<sup>14</sup>. All treatments are FDA-approved, though JR101's regimen is recommended but not preferred in NCCN guidelines. This analysis revealed distinct response patterns across molecular clusters (Fig. 1E):

- Cluster1/2: These clusters showed superior response to Ipi/Nivo with a 70% ORR in BIONIKK, significantly higher than the 42% ORR in the unselected CM214 population ( $p = 0.005$ ). In contrast, IO/TKI combinations showed no additional benefit—the 61% and 60% ORRs in KEYNOTE-426 and JR101 were comparable to the 56% ORR in

unselected CM9ER trial (both  $p > 0.4$ ), supporting the preferential use of IO/IO in angiogenic subtypes.

- Cluster4/5: Ipi/Nivo showed limited efficacy with similar ORRs in BIONIKK (41%) and CM214 (42%) ( $p = 1$ ). IO/TKI outcomes were mixed—JR101 showed a non-significant trend toward lower ORR (48%,  $p = 0.21$ ), while KEYNOTE-426 demonstrated modestly improved ORR (67%,  $p = 0.046$ ) compared to CM9ER (56%). This variability in IO/TKI responses warrants further investigation. Given the prevalence of epigenetic silencing through promoter hypermethylation in these clusters<sup>5</sup>, incorporating DNA hypomethylating agents might enhance immunotherapy efficacy<sup>15</sup>.

The molecular subtypes demonstrate both prognostic and predictive roles. Prognostically, cluster1/2 shows enrichment in favorable IMDC risk groups. More importantly, these subtypes demonstrate predictive value for treatment selection—angiogenic subtypes (clusters 1/2) show superior response specifically to IO/IO compared to unselected populations, while IO/TKI combinations provide negligible additional benefit.

This observation becomes particularly intriguing in the context of sarcomatoid features. While emerging data suggest immunotherapy is particularly effective for sarcomatoid RCC<sup>6</sup>, cluster1/2, which showed lower prevalence of sarcomatoid features, demonstrated superior response to IO/IO. This seemingly paradoxical observation aligns with recent retrospective data where IO/TKI combinations achieved higher response rates than IO/IO in sarcomatoid RCC (94% vs. 39%)<sup>16</sup>, suggesting molecular subtypes and histological features may independently influence treatment outcomes.

The underlying biology likely reflects complex interactions between angiogenesis and immunity. High angiogenesis in RCC may signify a tumor microenvironment where VEGF-driven immunosuppression is dominant<sup>17</sup>, but potentially reversible through dual checkpoint blockade. Tumors with extreme angiogenesis might develop compensatory mechanisms that allow T cell infiltration when combined with ICIs. Additionally, features like clonal neoantigens, tertiary lymphoid structures, and myeloid reprogramming might render these angiogenic tumors uniquely responsive to IO/IO<sup>18</sup>. This challenges the dogma by highlighting that angiogenesis-rich tumors are not merely “VEGF-addicted” but may instead rely on immune-evasion mechanisms that are more effectively targeted by ICIs than TKIs. Future mechanistic studies will be crucial to validate these hypotheses.

Several limitations warrant consideration. First, our focus on clusters 1, 2, 4, and 5 excludes clusters 3 and 6, which were less relevant for IO-based treatment selection given their non-significant differential responses between IO/TKI and sunitinib<sup>8</sup>, though this limits our evaluation to a narrower spectrum of molecular subtypes. Second, while bulk transcriptomics identifies distinct features between clusters (e.g., stromal/EMT characteristics in cluster 1), further studies should consider intra-cluster heterogeneity in the tumor microenvironment that may influence treatment responses. Third, while our findings advocate for reconsideration of using IO/IO in angiogenic mRCC, caution is advised due to variations in patient demographics and treatment protocols across different trials.

In summary, our study aims to critically evaluate the efficacy of IO/IO in treating mRCC across different molecular subgroups, particularly given the current absence of prospective trials directly comparing IO/IO and IO/TKI treatments. Moving forward, it is crucial to foster rigorous research efforts that not only challenge existing paradigms but also pave the way for more personalized and effective cancer care.

## Methods

### Sample collection and ethical approval

The BIONIKK study, registered under NCT02960906, is a biomarker-driven trial employing the Descartes classifications<sup>4</sup>. These classifications segregate four tumor types (crrcc1 to crrcc4) based on transcriptomic data that highlight varying responses to the drug sunitinib and different levels of immune and angiogenic activity within the tumor microenvironment.



Specifically, ccrcc4 tumors, less responsive to sunitinib, exhibit high immune and inflammatory activity with elevated checkpoint expression, whereas ccrcc1 tumors show minimal immune activity. Conversely, ccrcc2 tumors, which respond well to sunitinib, display robust angiogenic and immune activity, while ccrcc3 tumors resemble normal kidney tissue and also respond favorably to sunitinib<sup>19</sup>. All patients had previously provided informed consent for tumor collection and analysis, adhering to the ethical standards of the Declaration of Helsinki.

### Trial design and assessments

The efficacy of immunotherapy in advanced and/or metastatic clear cell renal cell carcinoma (ccRCC) was evaluated in several multi-center, open-labeled randomized controlled trials including BIONIKK (NCT02960906)<sup>4</sup>, KEYNOTE-426 (NCT02853331)<sup>10</sup>, JAVELIN Renal 101 (NCT02684006)<sup>12</sup>, CheckMate-214 (NCT02231749)<sup>14</sup>, and CheckMate-9ER (NCT03141177)<sup>14</sup>, all reported per CONSORT guidelines. We assessed the objective response rate (ORR) in patients treated with either immune-oncology (IO) combination therapies or IO plus anti-VEGF receptor tyrosine kinase inhibitors (VEGF-TKIs). The treatment regimens varied among the trials, with BIONIKK patients receiving nivolumab plus ipilimumab, KEYNOTE-426 participants given pembrolizumab plus axitinib, JAVELIN Renal 101 participants given avelumab plus axitinib, CheckMate-214 participants given nivolumab plus ipilimumab, and CheckMate-9ER participants given nivolumab plus cabozantinib. Additionally, Motzer's molecular subtypes were analysed or previously reported for trials with available RNA sequencing (RNA-seq) profiles to compare ORR across different trials.

### RNA sequencing

RNA-seq FASTQ files from 49 BIONIKK clinical trial samples treated with ipilimumab plus nivolumab underwent a rigorous quality control assessment using FastQC at both the base and read levels. Samples meeting quality standards were advanced to subsequent analyses. The STAR aligner, with default parameters and the GRCh38 reference genome, was used to generate RNA-seq BAM files<sup>20</sup>. Gene-level annotation employed GENCODE (Release 27), downloaded from the GENCODE project<sup>21</sup>. Aligned reads were summarized at the gene level using STAR, initially calculating the number of fragments per kilobase of non-overlapping exon per million fragments mapped, subsequently converted into transcripts per kilobase million (TPM) values.

### Classification of Motzer's molecular subtypes

Molecular subtypes, as identified in the IMmotion 151 trial, were reproduced using a template of significantly upregulated genes from Genentech's profiling on tumors from patients enrolled in the IMmotion151 study ( $\log_2\text{FoldChange} > 1.5$  and adjusted  $p\text{-value} < 0.05$ )<sup>3</sup>. Classification employed the nearest template prediction (NTP) method using  $\log_2$  transformed TPM values followed by z-score normalization to categorize each ccRCC case into corresponding subtypes based on predefined gene expression templates<sup>7,22</sup>. The NTP method was chosen over model-based machine learning approaches (e.g., random forest) for its flexibility and robustness, providing a model-free approach that adapts to varying datasets without the need for extensive parameter tuning or a perfect feature match. Molecular subtypes were previously reported on 369 and 357 samples in KEYNOTE-426 (pembrolizumab plus axitinib) and JAVELIN Renal 101 (avelumab plus axitinib), respectively<sup>8,11</sup>.

### Differential expression and pathway enrichment analysis

For differential expression analyses, the R package MOVICS<sup>23</sup> was used with the limma approach<sup>24</sup>, and for gene set enrichment analysis based on transcriptome expression data, a pre-ranked gene list was prepared according to the descending ordered  $\log_2\text{FoldChange}$  value derived from differential expression analysis, and used the R package clusterProfiler to determine functional enrichment based on the Hallmark pathways<sup>25</sup>.

### Statistical analysis

All statistical analyses were conducted using R version 4.2.2. Survival rates were analyzed using Kaplan-Meier curves, with differences determined using a log-rank test. Hazard ratios and 95% CI were calculated using Cox proportional hazard regression. For the comparison of ORRs across different treatment groups, Fisher's exact test was employed to determine statistical significance. A  $p\text{-value}$  less than 0.05 was considered statistically significant for all unadjusted analyses.

### Data availability

The raw data specific to the BIONIKK trial are not publicly available due to patient privacy regulations and the lack of authorization for distribution. Other data supporting the findings of this study are available from the corresponding author, G.M. (maloufg@igbmc.fr), upon request. Special inquiries regarding the BIONIKK trial data should also be directed to the corresponding author, who will coordinate these requests in accordance with the study sponsor's guidelines.

### Code availability

Analytic code supporting the findings of this study is available from the lead contact, G.M. (maloufg@igbmc.fr), upon request.

Received: 17 October 2024; Accepted: 17 April 2025;

Published online: 08 May 2025

### References

1. National Comprehensive Cancer Network. Kidney Cancer (Version 1.2025).
2. Motzer, R. J. et al. Molecular subsets in renal cancer determine outcome to checkpoint and angiogenesis blockade. *Cancer Cell* **38**, 803–817.e804 (2020).
3. Beckermann, K. et al. OPTimal Treatment by Invoking biologic clusters in renal cell carcinoma (OPTIC RCC). *Oncologist*. **28**(Suppl 1), S14 (2023).
4. Vano, Y. A. et al. Nivolumab, nivolumab-ipilimumab, and VEGFR-tyrosine kinase inhibitors as first-line treatment for metastatic clear-cell renal cell carcinoma (BIONIKK): a biomarker-driven, open-label, non-comparative, randomised, phase 2 trial. *Lancet Oncol.* **23**, 612–624 (2022).
5. Lu, X. et al. Silencing of genes by promoter hypermethylation shapes tumor microenvironment and resistance to immunotherapy in clear-cell renal cell carcinomas. *Cell Rep. Med.* **4**, 101287 (2023).
6. Bakouny, Z. et al. Integrative molecular characterization of sarcomatoid and rhabdoid renal cell carcinoma. *Nat. Commun.* **12**, 808 (2021).
7. Lu, X. et al. Racial disparities in MiT family translocation renal cell carcinoma. *The Oncologist* (2023).
8. Saliby, R. M. et al. Impact of renal cell carcinoma molecular subtypes on immunotherapy and targeted therapy outcomes. *Cancer cell* **42**, 732–735 (2024).
9. Motzer, R. J. et al. Biomarker analysis from CheckMate 214: nivolumab plus ipilimumab versus sunitinib in renal cell carcinoma. *J. Immunother.* *Cancer* **10**, e004316 (2022).
10. Rini, B. I. et al. Pembrolizumab plus axitinib versus sunitinib for advanced renal-cell carcinoma. *N. Engl. J. Med.* **380**, 1116–1127 (2019).
11. Rini, B. I. et al. Biomarker analysis of the phase 3 KEYNOTE-426 study of pembrolizumab (P) plus axitinib (A) versus sunitinib (S) for advanced renal cell carcinoma (RCC). *J. Clin. Oncol.* **42**, 4505–4505 (2024).
12. Motzer, R. J. et al. Avelumab plus axitinib versus sunitinib for advanced renal-cell carcinoma. *N. Engl. J. Med.* **380**, 1103–1115 (2019).
13. Choueiri, T. K. et al. Nivolumab plus cabozantinib versus sunitinib for advanced renal-cell carcinoma. *N. Engl. J. Med.* **384**, 829–841 (2021).

14. Motzer, R. J. et al. Nivolumab plus ipilimumab versus sunitinib in advanced renal-cell carcinoma. *N. Engl. J. Med.* **378**, 1277–1290 (2018).
15. Loo, Y. H. et al. DNA hypomethylating agents increase activation and cytolytic activity of CD8(+) T cells. *Mol. Cell* **81**, 1469–1483.e1468 (2021).
16. Fitzgerald, K. N. et al. Impact of sarcomatoid features on treatment outcomes in metastatic clear cell renal cell carcinoma treated with first-line immunotherapy combinations. *J. Clin. Oncol.* **41**, 687–687 (2023).
17. Fukumura, D., Kloepper, J., Amoozgar, Z., Duda, D. G. & Jain, R. K. Enhancing cancer immunotherapy using antiangiogenics: opportunities and challenges. *Nat. Rev. Clin. Oncol.* **15**, 325–340 (2018).
18. Jammihal, T. et al. Immunogenomic determinants of exceptional response to immune checkpoint inhibition in renal cell carcinoma. *Nat. Cancer* **6**, 372–384 (2025).
19. Beuselinck, B. et al. Molecular subtypes of clear cell renal cell carcinoma are associated with sunitinib response in the metastatic setting. *Clin. Cancer Res.* **21**, 1329–1339 (2015).
20. Dobin, A. et al. STAR: ultrafast universal RNA-seq aligner. *Bioinformatics* **29**, 15–21 (2013).
21. Harrow, J. et al. GENCODE: the reference human genome annotation for The ENCODE Project. *Genome Res* **22**, 1760–1774 (2012).
22. Hoshida, Y. Nearest template prediction: a single-sample-based flexible class prediction with confidence assessment. *PLoS One* **5**, e15543–e15543 (2010).
23. Lu, X., Meng, J., Zhou, Y., Jiang, L. & Yan, F. MOVICS: an R package for multi-omics integration and visualization in cancer subtyping. *Bioinformatics* **36**, 5539–5541 (2021).
24. Ritchie, M. E. et al. limma powers differential expression analyses for RNA-sequencing and microarray studies. *Nucleic Acids Res.* **43**, e47 (2015).
25. Wu, T. et al. clusterProfiler 4.0: A universal enrichment tool for interpreting omics data. *Innov. (N. Y)* **2**, 100141 (2021).

## Acknowledgements

This work was supported in part by grants from the Fondation ARC (SIGNIT) (G.M.). The funding agencies had no role in the study design; the collection, analysis, or interpretation of data; or the preparation, review, or approval of the manuscript for publication. The authors thank all the patients who participated in the clinical trials and whose data contributed to this study.

## Author contributions

X.L. and G.G.M. conceived and designed the study. X.L., Y.A.V., X.S., S.O., and G.G.M. acquired, analyzed, or interpreted the data. X.L., Y.A.V., and G.G.M. drafted the manuscript. All authors critically revised the manuscript for important intellectual content. X.L., X.S., and F.Y. performed the statistical analysis. G.G.M. obtained funding. W.H.F. and C.S.F. provided administrative, technical, or material support. S.O. and G.G.M. supervised the study. All authors reviewed and approved the final manuscript.

## Competing interests

The authors declare no competing interests.

## Additional information

**Supplementary information** The online version contains supplementary material available at <https://doi.org/10.1038/s41698-025-00912-x>.

**Correspondence** and requests for materials should be addressed to Stéphane Oudard or Gabriel G. Malouf.

**Reprints and permissions information** is available at <http://www.nature.com/reprints>

**Publisher's note** Springer Nature remains neutral with regard to jurisdictional claims in published maps and institutional affiliations.

**Open Access** This article is licensed under a Creative Commons Attribution-NonCommercial-NoDerivatives 4.0 International License, which permits any non-commercial use, sharing, distribution and reproduction in any medium or format, as long as you give appropriate credit to the original author(s) and the source, provide a link to the Creative Commons licence, and indicate if you modified the licensed material. You do not have permission under this licence to share adapted material derived from this article or parts of it. The images or other third party material in this article are included in the article's Creative Commons licence, unless indicated otherwise in a credit line to the material. If material is not included in the article's Creative Commons licence and your intended use is not permitted by statutory regulation or exceeds the permitted use, you will need to obtain permission directly from the copyright holder. To view a copy of this licence, visit <http://creativecommons.org/licenses/by-nc-nd/4.0/>.

© The Author(s) 2025